Global Science Research Journals

ISSN: 2465-7190 Vol. 7(1), pp. 217-222, January, 2019
©Global Science Research Journals
Author(s) retain the copyright of this article.
http://www.globalscienceresearchjournals.org/

Global Educational Journal of Science and Technology

Full Length Research Paper

An accurate numerical model for charge density in ballistic carbon nanotube field effect transistors (CNTFETs)

Bao-jun Liu[1], Li Cai[1], Xiaokuo Yang[1], Hongtu Huang[1], Xiaohui Zhao[1] and Ying Wen[2]

[1]Science Institute, Air Force Engineering University, Shanxi Xi'An, China, 710051.
[2]Engineering College, Air Force Engineering University, Shanxi Xi'An, China, 710038.

Abstract

Since the discovery of carbon nanotube (CNT), a great deal of groups pays more attention to it due to its unique properties. The theory of ballistic transport carbon nanotube field effect transistors (CNTFETs) is presented in the paper, and then a numerical model based on Newton-Raphson and linear approximation method for charge densities in CNTFET is proposed. The model could efficiently provide accurate solution to the self-consistent potential in a CNTFET, which is a function of parameters such as terminal voltages, CNT diameter, and Fermi level and so on. The model is simulated and the results show that compared with the piece-wise linear approximation, the numerical model in the paper is more accurate and efficient.

Keywords: Newton-Raphson method, ballistic carbon nanotube field effect transistors (CNTFETs), numerical model, self-consistent potential.

INTRODUCTION

Since the discovery of carbon nanotube (CNT) by Iijima in 1991 (McEuen, 2002), it has attracted more interests due to its unique electrical properties, such as reduced carrier scattering rate and high current carrying capability (Javey, 2003; Hichem, 2011; Pennington, 2005). And nowadays, a great deal of theoretical and experimental work has gone into understanding CNTs (Peng et al., 2006). CNTs are hollow seamless cylinders composed of one or more layers of grapheme sheets (Paul, 2007; Guo, 2007; Vitusecich, 2010). Depending on their chirality, they can be either semiconducting or metallic. Semiconducting CNT has been used in the high performance field effect transistor (FET) as the channel nanotube (Paul, 2007).

The electronic properties of CNTFET have been studied in theory and experiment (Peng et al., 2006). Ungersbǒck et al. (2003) simulated carrier transport in axial and lateral type CNTFETs and the simulation results show reasonable agreement with experimental data.

Dang et al. (2006) provided experimental data in detail and gave some compact models of CNTFETs. Deng et al. (2006) presented a circuit-compatible model of CNTFETs which can be simulated using HSPICE. The model can be well used in both digital and logic circuits (Liu, 2007). In their theory or simulation, the self-consistent potential is just approximately estimated, and they will not be in good agreement with experimental data when CNT parameters change. In other words, the device performance is a function of CNT parameters, such as diameter and length. To improve the device performance, Hashempour and Lombardi (2006) proposed a piece-wise linear approximation for self-consistent potentials in CNTFETs based on the ballistic transport theory. It can well accurately simulate CNTFETs, but the error between actual and modeled charge densities is a function of varied CNTFET parameters, such as CNT diameter and gate bias.

In order to effectively simplify the simulation of CNTFET, an accurate numerical model for charge density in CNTFETs is proposed in this paper based on ballistic transport theory (Dang, 2006; Hashempour and Lombardi, 2006; Rahman, 2003). The self-consistent potential of CNTFET is an important element in determining device current. So the more accurate self-consistent voltage compute, the less the error is. There are some advantage

*Corresponding author. E-mail: liubaojun102519@sina.com.

features in the proposed numerical model. Firstly, it provides a more accurate numerical model of charge density in CNTFETs. Next, it uses Newton-Raphson and linear approximation method to efficiently and accurately compute the self-consistent voltage, and the result is more close to the actual. Lastly, the model can be used in general applications and be realized in HSPICE.

Theory of ballistic CNTFET

The drain current of CNTFET has been computed by means of the ballistic theory (Dang, 2006; Hashempour and Lombardi, 2006; Rahman, 2003; Grado-Caffaro, 2008)

$$I_D = \frac{2q}{h}\int_{-\infty}^{+\infty} T(E)\,f(E-E_{FS}) - f(E-E_{FD})\,dE \quad (1)$$

where q is the electron charge, h is Planck's constant, $T(E)$ is the trace of the transmission matrix and $f(E)$ is the Fermi-Dirac occupation factor; E_{FS}, E_{FD} are the Fermi levels of the source and drain respectively, and $E_{FD} = E_{FS} - qV_{DS}$, where V_{DS} is the source-drain voltage.

Considering the first band contribution to the drain current, the drain current I_D can be formulated by

$$I_D = \frac{4qkT}{h}\ln\left(1+\exp\left(-\frac{U_{SCF}-E_{FS}}{kT}\right)\right) - \ln\left(1+\exp\left(-\frac{U_{SCF}-E_{FS}+qV_{DS}}{kT}\right)\right) \quad (2)$$

where T is the temperature, k is Boltzmann's constant, and U_{SCF} is the self-consistent potential in the first band.

From the Equation (2), specifying V_{DS} and E_{FS}, the drain I_D is just a function of the self-consistent potential. And *current* U_{SCF} is a function of CNTFET terminal voltages, deduced capacitances and conducting band potential, that is,

$$U_{SCF} = -q(\alpha_G V_G + \alpha_S V_S + \alpha_D V_D) + \frac{qN_1(U_{SCF}) + qN_2(U_{SCF}) - qN_0}{C_{tot}} \quad (3)$$

where

$$\alpha_G = \frac{C_G}{C_{tot}},\ \alpha_S = \frac{C_S}{C_{tot}},\ \alpha_D = \frac{C_D}{C_{tot}},\ C_{tot} = C_G + C_S + C_D,$$

and C_G, C_S, C_D are deduced capacitance of gate, source and drain, respectively. The mobile, source and drain charge densities represented by N_0, N_1 and N_2 are given by

$$N_0 = \int_0^{+\infty} \frac{D_0\,dz}{1+\exp\left(\frac{z^2+\varepsilon_1^2-\varepsilon_1-E_F}{kT}\right)} \quad (4)$$

$$N_1(U_{SCF}) = \int_0^{+\infty} \frac{\frac{D_0}{2}\,dz}{1+\exp\left(\frac{z^2+\varepsilon_1^2+U_{SCF}-\varepsilon_1-E_F}{kT}\right)} \quad (5)$$

$$N_2(U_{SCF}) = \int_0^{+\infty} \frac{\frac{D_0}{2}\,dz}{1+\exp\left(\frac{z^2+\varepsilon_2^2+U_{SCF}-\varepsilon_1-E_F+qV_{DS}}{kT}\right)} \quad (6)$$

where ε_1 denotes the first conducting band potential. $D_0 = \frac{8}{3\pi b V_{II}}$, where b is the carbon-carbon bond length, and $b = 0.142\text{nm}$, $V_{II} = 3e\text{V}$ represents the carbon-carbon bond energy.

An accurate numerical model

Hamidreza and Lombardi (2006) proposed a piece-wise linear model for Equations (4) to (6), however when the parameters change, such as CNT, diameter is smaller than 1 nm, the error is close to 10%, the model is not good enough to evaluate the self-consistent potential. Here, a numerical model combined Newton-Raphson method with linear approximation is proposed. The model can efficiently and accurately solve the Equation (3) by using mix methods, and the error is very low. Equation (3) can be rewritten by

$$F(x) = -q(\alpha_G V_G + \alpha_S V_S + \alpha_D V_D) + q\left(\frac{qN_1(x) + qN_2(x) - qN_0}{C_{tot}} - x\right) = 0 \quad (7)$$

The first step is to specify the initial self-consistent potential, such as $U_{SCF}^0 = 0$, and if $F(U_{SCF}^0) = 0$, the procedure is end with $U_{SCF} = U_{SCF}^0$, or else go to the second step.

The second step is to modify the initial self-consistent potential U_{SCF}^0 by $U_{SCF}^1 = U_{SCF}^0 + \Delta U_{SCF}^0$. The increment ΔU_{SCF} by means of Newton-Raphson method can be represented by

$$\Delta U_{SCF}^0 = -\frac{F(U_{SCF}^0)}{\left.\frac{dF}{dx}\right|_{U_{SCF}^0}} \quad (8)$$

where $\frac{dF}{dx}$ is equated to $\frac{q^2}{C_{tot}}\left(\frac{dN_1}{dx}+\frac{dN_2}{dx}\right) - 1$, and

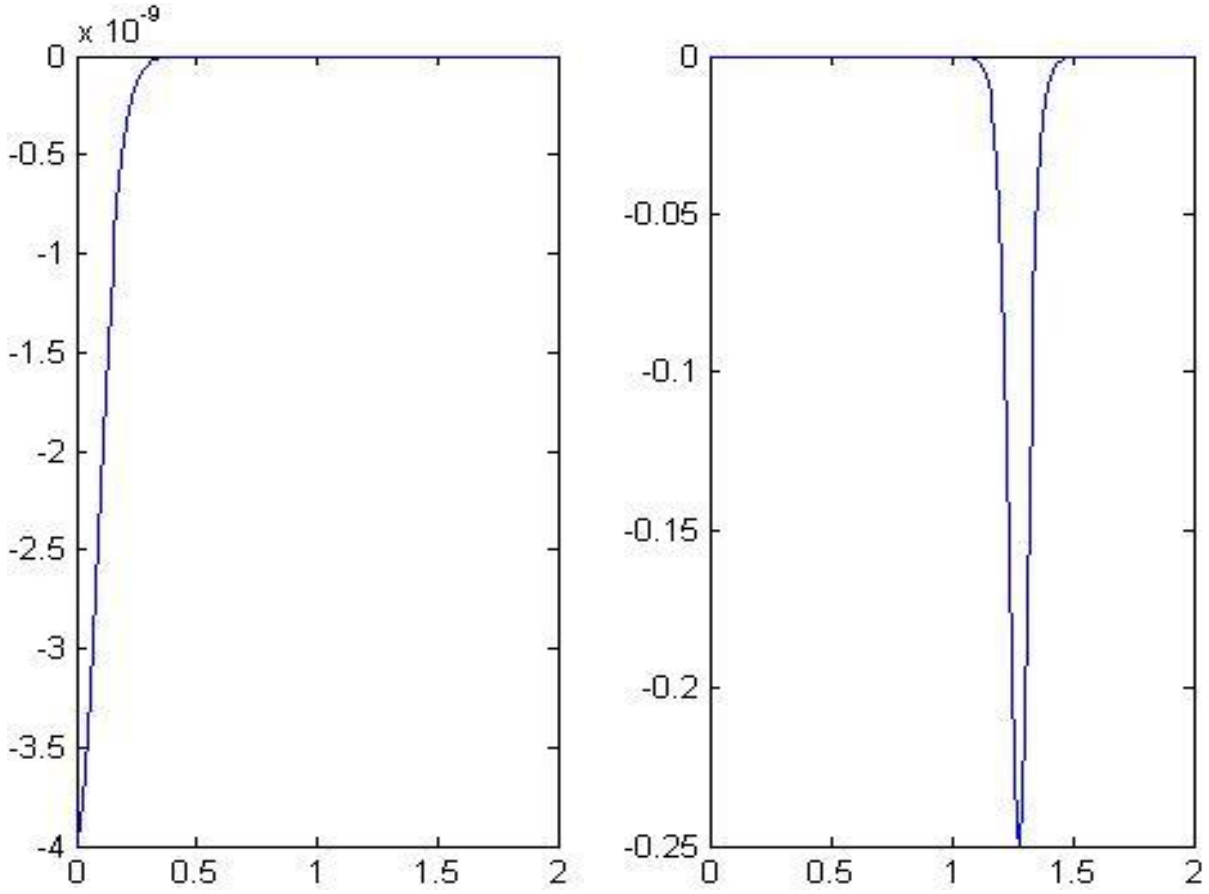

Figure 1. Integral function with different parameters.

$$\frac{dN_1}{dx} = \int_0^{+\infty} \frac{D_0}{2kT} f_1(z)\,dz = \int_0^{+\infty} \frac{\frac{D_0}{2kT}\exp\left(\frac{\sqrt{z^2+\varepsilon_1^2}+x-\varepsilon_1-E_{F_S}}{kT}\right)}{\left(1+\exp\left(\frac{\sqrt{z^2+\varepsilon_1^2}+x-\varepsilon_1-E_{F_S}}{kT}\right)\right)^2}\,dz \quad (9)$$

$$\frac{dN_2}{dx} = \int_0^{+\infty} \frac{D_0}{2kT} f_2(z)\,dz = \int_0^{+\infty} \frac{\frac{D_0}{2kT}\exp\left(\frac{\sqrt{z^2+\varepsilon_1^2}+x-\varepsilon_1-E_{F_S}+qV_{DS}}{kT}\right)}{\left(1+\exp\left(\frac{\sqrt{z^2+\varepsilon_1^2}+x-\varepsilon_1-E_{F_S}+qV_{DS}}{kT}\right)\right)^2}\,dz \quad (10)$$

Actually, Equations (9) and (10) are hard to get the numerical integral. Here, an area approximation is used to estimate the numerical value instead of integral. Figure 1 is the integral function of Equation 9 with different parameters. Their difference is just that the maximum value of the function in the left falls in the origin and in the right falls in other point. From Figure 1, it is known that the numerical integral of the Equation (9) is just the approximative triangle's area. And for Equation 9, the area can be represented by

$$\frac{dN_1}{dx} = \frac{D_0}{2kT}\left(\frac{1}{2}ab\right) \quad (11)$$

where a is the width of the triangle, and b is the maximum value of the function. And b can be evaluated by

$$b = \begin{cases} f_1(z_m), & if \quad x \le E_{F_S} \;\&\&\; x \le E_{F_S} + \varepsilon_1 \\ f_1(0), & others. \end{cases} \quad (12)$$

$$z_m = \left(x - E_{F_S} - \varepsilon_1\right)^2 - \varepsilon_1^2 \quad (13)$$

Assume a measure of closeness as $\varepsilon = 5\times10^{-5} b$, then if $f_1(x)$ is close to 0, we have the zero points. And a can be represented by

$$a = \begin{cases} z_1 - z_2, & if x \le E_{F_S} \;\&\&\; x \le E_{F_S} + \varepsilon_1 \\ \varepsilon_1, & others. \end{cases} \quad (14)$$

$$z_1 = \left(kT\ln(k_1) + E_{F_S} + \varepsilon_1 - x\right)^2 + \varepsilon_1^2 \quad (15)$$

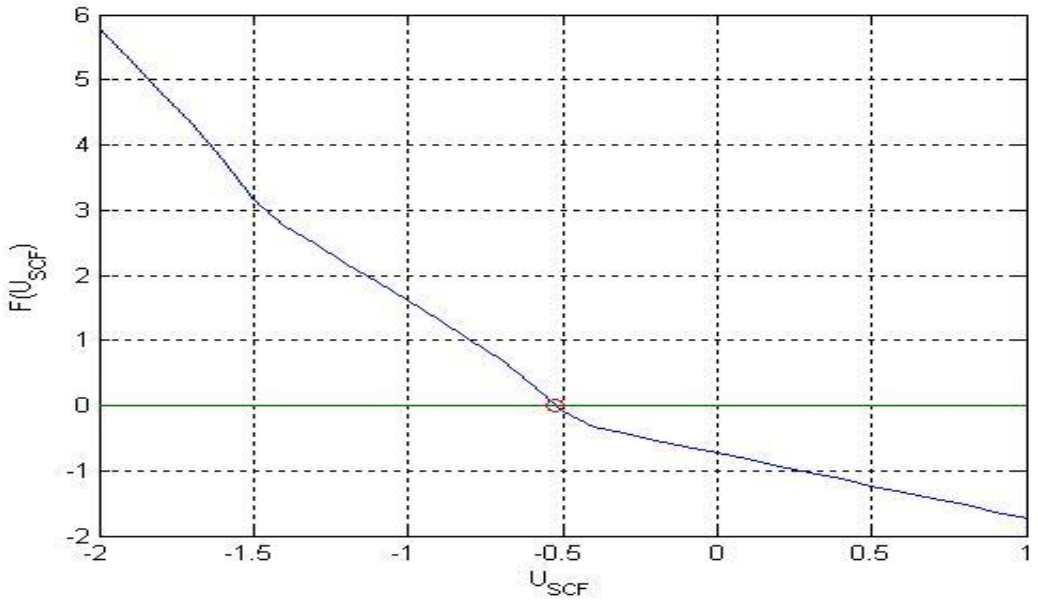

Figure 2. Graphic $F(U_{SCF})$.

$$z_2 = (k\sqrt{T}\ln(k_2) + E_F + {}_s - {}_1 - x)^2 + {}_1^2 \quad (16)$$

where k_1 and k_2 are the function of ε as

$$k_1 = \frac{1 - 2\varepsilon + \sqrt{-4\varepsilon}}{2\varepsilon} \quad (17)$$

$$k_2 = \frac{1 - 2\varepsilon - \sqrt{1 - 4\varepsilon}}{2\varepsilon} \quad (18)$$

From Equations (11) to (18), $\frac{dN_1}{dx}$ can be approximately evaluated. And just replace E_F with $E_{F_S} - qV_{DS}$ between Equations (11) and (18) to evaluate $\frac{dN_2}{dx}$.

By Newton-Raphson method, the third step is to calculate $F(U_{SCF}^1)$, and compare $F(U_{SCF}^1)$ with a small number ξ, such as $\xi = 5 \times 10^{-4}$. If $F(U_{SCF}^1)$ issmaller than ξ, the procedure ends, or else go to the second step with $U_{SCF}^2 = U_{SCF}^1 + U_{SCF}^1$, where U_{SCF}^1 can be evaluated by Equation 8 by replacing U_{SCF}^0 with U_{SCF}^1. The iteration goes on with

$$U_{SCF}^{k+1} = U_{SCF}^k + U_{SCF}^k = U_{SCF}^k - \frac{F(U_{SCF}^k)}{\left.\frac{dF}{dx}\right|_{U_{SCF}^k}} \quad (19)$$

And when $F(U_{SCF}^{k+1})$ is smaller than ξ, the iteration ends with $U_{SCF} = U_{SCF}^{k+1}$.

RESULTS AND DISCUSSION

Here, the aforementioned numerical model will be simu-lated, and Hashempour and Lombardi (2006) proposal that a piece-wise linear model will also be modeled just to be compared with our model about performance. The simulation parameters are set as follows; the temperature is 300 K, CNT diameter is $d = 1.4246\text{nm}$, the source Fermi level E_{F_S} is set to -0.5eV, and $V_G = 0.8\text{V}$, $V_{DS} = 0.8\text{V}$, ${}_1 = 0.45/d$ eV. From [17], α_G, α_S, α_D are0.87, 0.097, 0.033, respectively, and C_{tot} is 90 pF. Firstly, the graphic method is used to solve Equation 7. Figure 2 shows that the function $F(U_{SCF})$ varies with U_{SCF}, and the answer of Equation 7 is the point where $F(U_{SCF})$ intersect with $F = 0$, as red circle in Figure 2. By using the graphic method, a close to actual answer could be gotten whose error is lower than10^{-6}, but it spends more time to get the answer, and the integral also needs more computer time. Figures 3 and 4 show the simulation results where 'N-R' and 'P-W-L' represent the Newton-Raphson method and piece-wise linear method, respectively. The relative error is the self-consistent potentials gotten from above methods compare with one

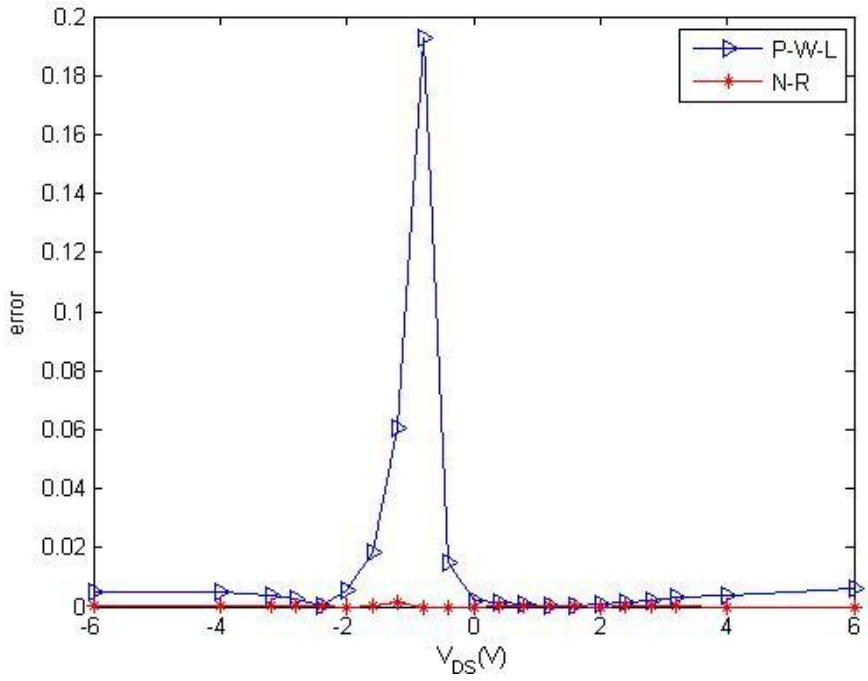

Figure 3. The relative error with different source-drain voltage.

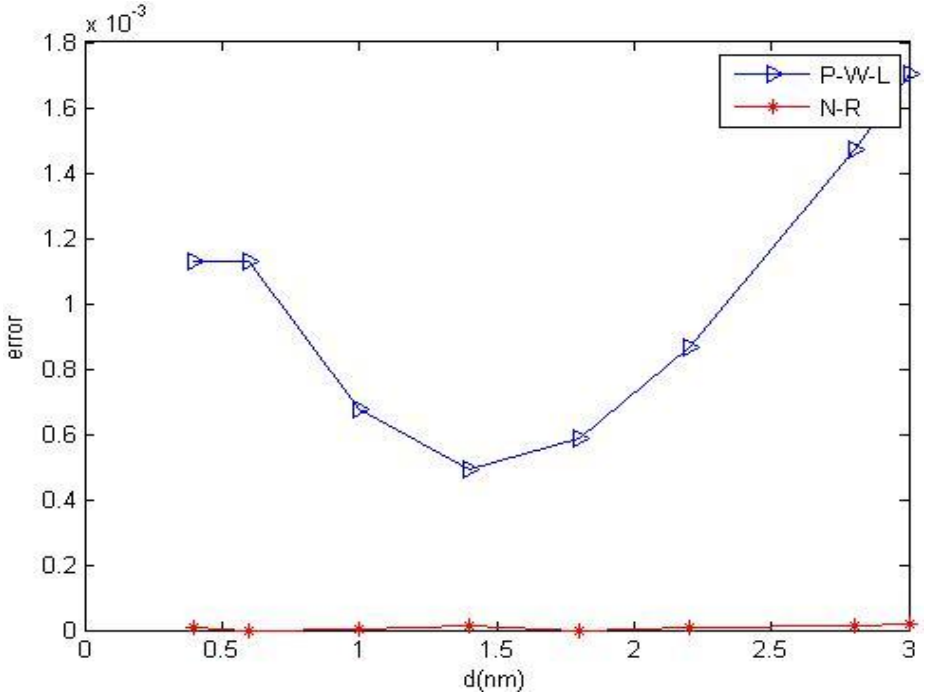

Figure 4. The relative error with different CNT diameters.

from graphic method based on the same parameters. In Figure 3, the relative error of N-L method is close to zero whatever the source-drain voltage varies. However, the relative error of P-W-L method varies as the source-drain voltage changes and when $V_{DS} = -0.8V$, the relative error is top to 19.5%. In Figure 4, when CNT diameter is ranging from 0.4 to 3 nm, the relative error of N-L method is lower than 0.2×10^{-4}, while the relative error of P-W-L method almost achieves to 0.0017, which is remarkable bigger than N-L method's. When CNT diameter belongs to the

range from 1 to 2 nm, the relative error of P-W-L method is lower than 0.001. From Figures 3 and 4, it can be concluded that the self-consistent potential is more accurate and efficient by using N-L method than by using P-W-L method.

Conclusion

In the paper, the theory of ballistic transport in CNTFETs is introduced and the charge density model is represented. In order to get the more accurate self-con-sistent potential efficiently, a numerical model is proposed by combining Newton-Raphson method with area approxi-mation and is simulated. From simulation result, it indicates that the numerical model can accurately and efficiently evaluate the self-consistent potential of CNTFETs. With the development of EDA technology, the numerical model can be realized by using HSPICE.

ACKNOWLEDGEMENTS

This work was supported in part by: The National Science Foundation of China under Grant No. 61172043; the Key Program of Shaanxi Provincial Natural Science for Basic Research under Grant No. 2011JZ015; Research Fund of Shaanxi Key Laboratory of Electronic Information System Integration under Grant No. 201115Y15, and Graduate Student Science and Technology Innovation Program of Air Force Engineering University under Grant No. Dx2010404.

REFERENCES

Dang T, Anghel L, Leveugle R (2006). CNTFET basics and simulation. In IEEE Int. Conf. Des. Test Integ. Sys. Nanoscale. Tech., pp. 1-6.

Deng J, Wong HSP (2007). A compact SPICE model for carbon nanotube field-effect transistors including nonidealities and its application- part I: model of the intrinsic channel region. IEEE Trans. Elec. Dev., 54(12): 3186-3194.

Grado-Caffaro MA, Grado-Caffaro M (2008). On ballistic transport in carbon nanotubes. Optik, 119: 601-602.

Guo J, Muhammad AA, Ouyang Y (2007). Subband gap impact ionization and excitation in carbon nanotube transistors. J. Appli. Phys., 101: 064311.

Hashempour H, Lombardi F (2006). An efficient and symbolic model for charge densities in ballistic carbon nanotube FETs. IEEE Nano. 1: 17-20.

Hichem T, Abdelkader M (2011). New extraction method of the scattering parameters of a physical system starting from its causal bond graph model: Application to a microwave filter. Int. J. Phys. Sci., 6(13): 3016-3030.

Javey A, Guo J, Wang Q, Lundstrom M, Dai H (2003). Ballistic carbon nanotube field-effect transistors. Nature. 424: 654-657.

McEuen PL, Fuhrer MS, Park H (2002). Single-walled carbon nanotube electronics. IEEE Trans. Nanotech., 1(1): 78-85.

Paul BC, Fujita S, Okajima M, Lee T (2007). Prospect of ballistic CNTFET in high performance applications: modeling and analysis. ACM J. Emerg. Tech. Comput. Sys., 3(3):12.

Peng GW, Huan ACH, Liu L, Feng YP (2006). Structural and electronic properties of 4 A^{0} carbon nanotubes on Si (001) surfaces. Phys. Rev., B. 74: 235416.

Pennington G, Goldsman N (2005). Low-field semiclassical carrier transport in semiconducting carbon nanotubes. Phys. Rev., B. 71: 205318.

Rahman A, Guo J, Datta S, Lundstrom MS (2003). Theory of ballistic nanotransistors. IEEE Trans. Elec. Dev., 50(9): 1853-1864.

Ungersbŏck E, Andreas Gehring, Hans Kosina, Siegfried Selberherr, Byoung-Ho Cheong, Won Bong Choi (2003). Simulation of Carrier Transport in Carbon Nanotube Field Effect Transistors. http://www.imec.be/esscirc/essderc-esscirc-2003/papers/all/545.pdf

Vitusecich SA, Sydoruk VA, Petrychuk MV, Danilchenko BA, Klein N, Offenhăusser A，Ural A, Bosman G (2010). Transport properties of single-walled carbon nanotube transistors after gamma radiation treatment. J. Appli. Phys. 107: 063701.

Wang S, Grifoni M (2007). Schottky-barrier double-walled carbon-nanotube field effect transistors. Phys. Rev., B. 76: 033413.